GLUCOSE-INDUCED OSCILLATORY CHANGES IN EXTRACELLULAR IONIZED POTASSIUM CONCENTRATION IN MOUSE ISLETS OF LANGERHANS

ELIA PEREZ-ARMENDARIZ, ILLANI ATWATER, AND EDUARDO ROJAS
Laboratory of Cell Biology and Genetics, National Institute of Arthritis, Diabetes, and Digestive and Kidney Diseases, National Institutes of Health, Bethesda, Maryland 20205; and Department of Biophysics, School of Biological Sciences, University of East Anglia, Norwich NR4 7TJ, United Kingdom

ABSTRACT Liquid membrane $[K^+]$-sensitive microelectrodes (1–2 μm tip diameter) were used to measure the extracellular ionized potassium concentration in mouse pancreatic islets of Langerhans. With the tip of the microelectrode at the surface of the islet, the time course of the $[K^+]$-sensitive electrode potential changes in response to the application of rapid changes in $[K^+]_o$ (from 1.25 to 5 mM), could be reproduced by the equation for K^+-diffusion through a 100-μm-thick unstirred layer around the islet (diffusion coefficient for K^+ at 27°C, $D_{K,o}$, taken as 1.83×10^{-5} cm^2/s). The time to reach 63% of the steady-state electrode response with the tip in the chamber at the surface of the islet was from 5 to 6 s. When the tip of the $[K^+]$-sensitive electrode was placed in the islet tissue, the time for the response to reach 63% of the steady-state level increased. The time course of the $[K^+]$-sensitive electrode response could be reproduced using the same diffusion model assuming that K^+ diffusion into the islet tissue takes place in a tortuous intercellular path with an apparent diffusion coefficient, $D_{K,I}$, about half of $D_{K,o}$, in series with the unstirred layer around the islet. In the absence of glucose the potassium concentration in the extracellular space, $[K^+]_I$, was found to be higher than the concentration in the external modified Krebs solution, $[K^+]_o$. The difference in concentration $[K^+]_I - [K^+]_o$ was greater when $[K^+]_o$ was smaller than 2 mM. In the presence of glucose (between 11 and 16 mM), under steady-state conditions, small oscillatory changes in the $[K^+]_I$ (1.48 ± 0.94 mM) were detected. Simultaneous recording of membrane potential from one B-cell and $[K^+]_I$ in the same islet indicated that the potassium concentration increased during the active phase of the bursts of electrical activity. Maximum concentration in the intercellular was reached near the end of the active phase of the bursts. We propose that the space between islet cells constitutes a restricted diffusion system where potassium accumulates during the transient activation of potassium channels.

INTRODUCTION

Studies of the periodic burst pattern of electrical activity induced by glucose in the pancreatic B-cell have indicated that the underlying mechanism involves the cyclic activation of a K^+-permeability that is modulated by intracellular Ca^{2+}, $P_K - [Ca^{2+}]_i$ (Atwater et al., 1979; Atwater et al., 1983). Furthermore, it is well documented that the action potentials during the bursts result from the activation of two voltage-gated membrane channels. Ca^{2+} channels (Matthews and Sakamoto, 1975; Atwater et al., 1978; Ribalet and Beigelman, 1980) and K^+ channels (Atwater et al., 1979*b*). Since the endocrine cells of a single islet of Langerhans from mouse have been shown to be electrically coupled (Eddlestone et al., 1984), and for the most part, synchronous throughout the islet (Meda et al., 1984), and since the intercellular space within the islet is rather limited (Dean, 1973), it is likely that the extracellular concentration of the ions involved in the electrical activity undergo fluctuations concomitant with the burst pattern.

We report here the results of experiments designed to measure ionized potassium in the intercellular spaces of the islet of Langerhans from mouse using $[K^+]$-sensitive microelectrodes. The results indicate that the diffusion coefficient for K^+ in the islet space is about one half of that of K^+ in the solution. In absence of glucose, basal $[K^+]_I$ is higher than $[K^+]_o$ indicating accumulation of K^+ in the islet extracellular space. Further, small oscillations in $[K^+]_I$ were detected in the presence of 11 mM glucose, which were simultaneous with bursts of electrical activity recorded from a cell in the same islet.

METHODS

Membrane Potential Measurements on Single Microdissected Mouse Islets of Langerhans

The electrophysiological methods that were used in this work have been described before (Atwater et al., 1978).

The volume of the chamber was 0.04 cm^3 (40 μl) and the rate of perfusion was 2.5 cm^3/min (42 μl/s). When changing solution at the stopcock (Kilb and Stämpfli, 1974), the new solution reached the chamber 2 s after the switch.

The modified Krebs solution used during the experiments had the following composition: 120 mM NaCl, 25 mM $NaHCO_3$, 5 mM KCl, 2.5 mM $CaCl_2$, and 1.1 mM $MgCl_2$ and was equilibrated with 95:5% O_2/CO_2 at 37°C.

Potassium-selective Microelectrodes

$[K^+]$-selective microelectrodes were made according to the technique described by Thomas (1978) and Tsien and Rink (1980). First, the microelectrodes were silanized with *N,N*-dimethyl-trimethylsilylamin (Fluka Chemical Corp.) vapor at 200°C. Next, the $[K^+]$-selective liquid membrane electrode was prepared by back-filling the microelectrode with the reference 100 mM KCl solution first, and then sucking into the tip of the microelectrode a column of ~250 μm of the liquid resin (Corning 477317; Corning Medical, Corning Glass Works, Medfield, MA, generously provided by Dr. R. Thomas). The resistance of the final electrode ranged between 0.5 and 1.5 GΩ.

The solution in the chamber was electrically connected to earth potential with an Ag/AgCl wire via a 1,000 Ω resistor. The reference electrode was made with another Ag/AgCl wire inside an agar bridge placed in the chamber. To measure the rising time of the $[K^+]$-sensitive electrode response to a voltage step, voltage pulses were applied to the solution in the chamber through the Ag/AgCl wire. When a rectangular voltage pulse was applied to the tip of a 1.5 GΩ $[K^+]$-sensitive electrode in solution, 63% of the applied voltage pulse was reached in <0.2 s.

Calibration of the Microelectrode and Controls

The $[K^+]$-selective microelectrodes used were calibrated before and after each experiment. To calibrate the electrode a modified K-Krebs solution was prepared (150 mM K^+ in place of Na^+) and mixed with Na-Krebs solution (0 mM K^+) to give the desired $[K^+]_o$, but with the sum $[K^+]_o$ + $[Na^+]_o$ and all other ions constant.

The responses of the $[K^+]$-electrode to modified Krebs solutions of decreasing and increasing concentration of $[K^+]_o$ (from 100 to 1.25 mM) are shown in Fig. 1. The $[K^+]$-sensitive electrode potentials are plotted as a function of the logarithm of the external potassium concentration; the curve, drawn to fit the points, was calculated using the Goldman-Hodgkin-Katz equation (Goldman, 1943; Hodgkin and Katz, 1949), which is more familiar to physiologists than the nomenclature of ion-selective electrodes (Commission on Analytical Nomenclature, 1976). The potential at the tip of the liquid membrane electrode becomes

$$V_K = V_o + RT/F \ln ([K]_o + SC\,[Na]_o), \quad (1)$$

where SC represents the selectivity ratio P_{Na}/P_K for the liquid membrane and RT/F equals 25.85 mV at 27°C. Since the reference solution inside the liquid membrane electrode was 100 mM, V_o was obtained from Eq. 1 when $[K]_o$ is 100 mM. Two parameters are needed to characterize the ion-sensitive electrode response: V_o and SC. V_o and SC values ranged from −115 to −125 mV and 0.01 to 0.05 mV respectively for different electrodes and remained constant for each electrode during the experiments. Experimental procedures, like changes in glucose concentration from 0 to 22 mM and increasing the concentration of $CaCl_2$ from 2.5 to 7.5 mM, did not change V_o or SC.

Since zinc is released together with insulin during exocytosis, the extracellular concentration of zinc during secretion may reach 25 μM (Ferrer, Soria, Dawson, Atwater, and Rojas, 1984). Therefore, we also tested the effects of 250 μM $ZnCl_2$ on these parameters. The values of V_o and SC were unchanged in the presence of Zn^{2+}.

Another experimental manipulation used to minimize any possible interferences due to the process of insulin release, was to perform experiments at 27°C. At this temperature insulin release from mouse islets is blocked while electrical activity continues (Atwater, Goncalves, Herchuelz, Lebrun, Malaisse, Rojas, and Scott, 1984). It was found that lowering the temperature from 37 to 27°C reversibly changes V_o from −119.9 to −114.6 mV and SC from 0.028 to 0.018. Thus, at 27°C the K^+ selectivity of the electrode increased in the low concentration range.

It may also be concluded that experimental manipulations in the concentration of glucose, $[Ca^{2+}]_o$ and $[Zn^{2+}]_o$ did not affect the overall response of the electrode.

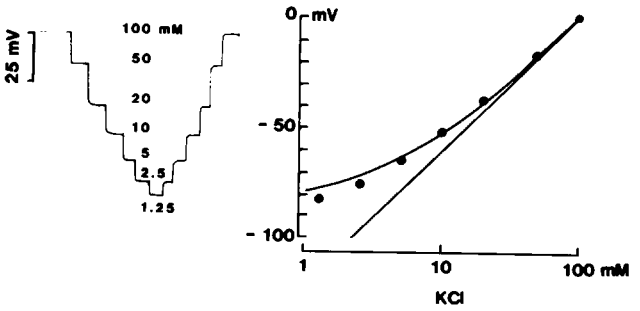

FIGURE 1 Calibration of the $[K^+]$-sensitive microelectrode. *Left* side: chart recording of the $[K^+]$-sensitive electrode potential V_K. $[K^+]_o$ in the chamber is indicated on the record. The switch from 2.5 to 1.25 mM and back to 2.5 mM took 1 min. Temperature 27°C. *Right* side: V_K as a function of $[K^+]_o$ (in semi-logarithmic scale). The straight line represents the Nernst potential and the fitted curve was calculated as explained in the text. From the fit the following microelectrode parameters were obtained: V_o = −119.3 mV and SC = 0.025.

Estimation of the Penetration Depth

The $[K^+]$-sensitive electrode was mounted vertically while the intracellular electrode was mounted at an angle of 70° from vertical to allow the electrodes to be brought close together without interference between their carriers. The final approach to the tissue with the $[K^+]$-sensitive electrode was observed under a magnification of 100. The penetration depth was estimated using the calibrated micrometer in the micromanipulator.

RESULTS

Time Course of the $[K^+]$-sensitive Electrode Response During a Sudden Change of $[K^+]$ in the External Medium

The time courses of the responses of the $[K^+]$-sensitive electrode (V_K) to a sudden elevation of the external K^+ concentration (from now on referred to as $[K^+]_o$) from 1.25 to 5 mM and to a sudden decrease back to 1.25 mM are shown in the upper part of Fig. 2. The responses obtained with the microelectrode tip within the islet tissue (dashed lines) were displaced along the voltage axis to achieve a common start with the response obtained at the surface of the islet (continuous lines) to facilitate the comparison. For the small changes in $[K^+]_o$ as illustrated in Fig. 2, the time courses of the $[K^+]$-sensitive microelectrode responses V_K were similar to the time courses of $[K^+]_o$. This was true despite the fact that the $[K^+]$-sensitive microelectrode potentials are logarithmically related to the $[K]_o$. Therefore, the traces in Fig. 2 are good descriptions of the time course of the $[K^+]$ change.

In the absence of glucose at 27°C, the average time for

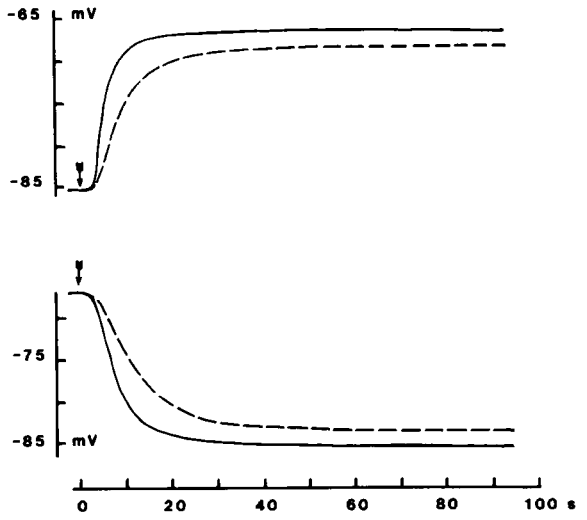

FIGURE 2. Time course of the [K⁺]-sensitive microelectrode response. Solid records (and vertical calibration): tip of the [K⁺]-sensitive microelectrode on the surface of the islet. The time from the beginning of each record to the arrow indicates the estimated transit time from the stopcock to the chamber. Dashed records: tip 56 μm inside the islet. Krebs solution without glucose at 27°C. *Upper* part: superimposed tracings of the time course of V_K after a switch from 1.25 to 5 mM K^+. Dashed record was shifted along the voltage axis from −81.5 (measured inside the islet) to −85.1 mV (measured with the electrode on the surface of the islet). *Lower* part: superimposed tracings after a switch from 5 to 1.25 mM K^+. V_K in 5 mM K^+, −64.5 mV for the dashed record. The arrows indicate the estimated delay from the time of the switch at the stopcock (beginning of the record).

V_K at the surface of the islet, to achieve 63% of the steady-state level following a sudden increase in $[K^+]_o$ from 1.25 to 5 mM was ~6.3 s. With the tip 56 μm within the islet tissue, the average time required for V_K to reach 63% of the steady-state value of increased to ~10.5 s. The time course of the [K⁺]-sensitive electrode responses to sudden changes in $[K^+]_o$ were, in most respects, similar to the records shown in Fig. 2 regardless of the duration of the experiments (<30 min).

Another interesting result in Fig. 2 is the difference between the steady-state levels of the potentials recorded by the [K⁺]-sensitive electrode inside the islet with respect to the levels recorded in solution at either 1.25 or 5 mM $[K^+]_o$. This result is analyzed in more detail later on (see Fig. 7).

Apparent K^+-diffusion Coefficient in the Intercellular Islet Spaces

If the [K⁺]-sensitive electrode monitored the concentration of K^+ in the intercellular space ($[K^+]_I$), it was possible to estimate the K^+ exchange between the intercellular space and both the intracellular compartment (mostly B-cells) and the external solution. There are two ways to estimate an apparent diffusion coefficient from records like those shown in Fig. 2: First, using a diffusion model (see Discussion) to generate the time course of $[K^+]_I$ and, second, from the change in time required for $[K^+]_I$ to reach 63% of the maximum response of the [K⁺]-sensitive electrode.

Although the shape of the islets examined was not spherical (largest islet diameter ranged from 150 to 250 mm: smallest diameter ranged from 100 to 150 μm), the diffusion model was based on radial diffusion into a spherical islet (180 μm radius) through a 100-μm–thick unstirred layer. The calculated time course of the [K⁺]-sensitive microelectrode response V_K (continuous line) when $[K^+]_o$ was augmented from 5 to 10 mM is compared with the experimental data in Fig. 3 (see Discussion). The diffusion coefficient in the solution, $D_{K,o}$ was taken as 1.83×10^{-5} cm²/s (Robinson and Stokes, 1959) and the thickness of the unstirred layer around the islet was adjusted to 100 μm.

Shown in the upper part of Fig. 3 are the V_K values (•) obtained with the microelectrode at the surface of the islet. The continuous curve was calculated to fit the experimental points. It may be seen that, the time course calculated assuming a 100-μm–thick unstirred layer was similar to the time course of the [K⁺]-sensitive microelectrode response. The time to 63% of the maximum response was calculated as 5.1 s. The measured response (•) and the predicted time course with the tip 28 μm within the islet tissue are shown in the lower part of Fig. 3. Also shown in the lower part (for reference) is the curve calculated to fit

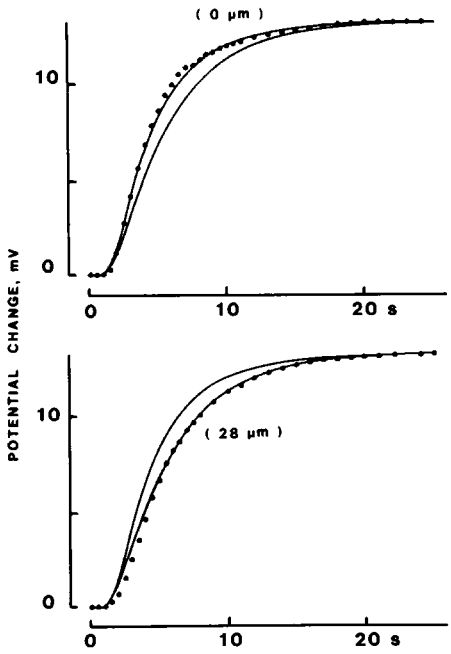

FIGURE 3 Comparison between the experimental and theoretical [K⁺]-sensitive microelectrode responses. Continuous curves represent calculated responses. Points represent V_K values obtained with the electrode on the surface of the islet (*upper* part) and with electrode at a depth of 28 μm into the islet tissue (*lower* part). Experimental points obtained in the islet were normalized to the voltage response of the electrode outside the islet tissue shown in the upper part. Change in $[K^+]_o$ from 5 to 10 mM. Islet in the absence of glucose at 27°C. Parameters for calculated curves: thickness of the unstirred layer equal to 100 μm; $D_{K,o} = 1.83 \times 10^{-5}$ cm²/s (curve fitted to the points in the upper part); $D_{K,I} = 0.9 \times 10^{-5}$ cm²/s.

the experimental points recorded with the electrode at the surface of the islet. The predicted response 28 μm inside the islet tissue was calculated by adjusting the apparent diffusion coefficient for K^+ in the intercellular spaces to minimize the residual

$$R = \Sigma \Delta V^2,$$

where ΔV represents the difference between measured and predicted values. The apparent diffusion coefficient in the islet extracellular space ($D_{K,I}$) from the fit was 0.9×10^{-5} cm^2/s and the calculated time to 63% of the response is 6.1 s.

It is also possible to estimate the apparent diffusion coefficient from the following relation

$$D_{K,I} = \Delta r^2/\Delta T, \quad (2)$$

where Δr is the radial distance from the tip of the electrode to the surface and ΔT is the difference between the time for the response to reach 63% of the steady-state level at Δr and the time required to reach the same relative response at the surface (Crank, 1956), i.e., ΔT is a measure of the time for K^+ to diffuse into the islet through the intercellular clefts. As Δr was 28 μm the apparent diffusion coefficient, $D_{K,I}$, was calculated as 0.78×10^{-5} cm^2/s. For the experiment shown in Fig. 2, Δr was 56 μm and ΔT was 4.2 s for the change from 1.25 to 5 mM and 4.5 s for the reverse change. The apparent diffusion coefficient, $D_{K,I}$, was 0.75×10^{-5} cm^2/s.

The two estimates of the diffusion coefficient based on the data in Fig. 3, were quite similar. In five other experiments (in which Δr ranged from 28 to 84 μm and ΔT from 1.0 to 6.5 s) in three different islets, the $D_{K,I}$ value estimated by either method was about half of that of $D_{K,o}$.

Oscillatory Changes in the Intercellular Concentration of Potassium in the Presence of Glucose

In the presence of glucose, between 8 and 16 mM, cyclic changes in B-cell membrane K^+-permeability occur (Atwater et al., 1978). The duration of the active phase depends on the Ca^{2+} entry during the active phase of the bursts, since progressive stimulation of the $[Ca^{2+}]_i$-activated K^+-permeability causes membrane hyperpolarization and termination of the burst. However, during the action potentials along the active phase of the bursts, voltage-gated K^+-channels are activated and could contribute to an increase in $[K^+]_I$. In the following experiments, each semidissected islet was first exposed to 11 mM glucose, the $[K^+]$-sensitive electrode was slowly introduced into the islet tissue, and then a B-cell was impaled with a high resistance microelectrode.

The effects of 11 mM glucose on $[K^+]_I$ and on B-cell membrane potential in the same islet are shown in Fig. 4. Note that the cell responded to 11 mM glucose with the characteristic burst pattern of electrical activity. The

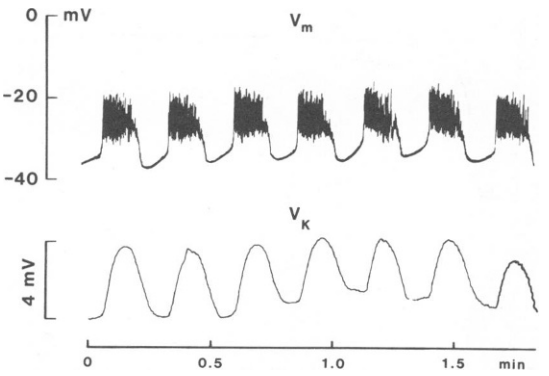

FIGURE 4 Simultaneous recordings of the intracellular potential, V_m, and the $[K^+]$-sensitive microelectrode potential, V_K. V_m represents the membrane potential record from a cell ~20 μm from the surface of the islet. V_K represents the $[K^+]$-sensitive microelectrode potential record made with the tip at a depth of ~65 μm. The microelectrode tips were separated by ~110 μm. Islet perifused with Krebs solution plus 11 mM glucose at 37°C. Mean amplitude of V = 3.5 ± 0.3 mV; Mean amplitude of $[K^+]_I$ = 1.5 ± 0.1 mM; Mean value for the initial rate of change dV_K/dt = 1.8 ± 0.4 mV/s; Mean value for the initial concentration change $d[K^+]_I/dt$ = 0.8 ± 0.2 $\mu M/cm^3 s$ (n = seven oscillations).

record of the $[K^+]$-sensitive microelectrode response (record labeled as V_K) exhibited cyclic changes in phase with the bursts of electrical activity.

Similar oscillations in V_K were recorded from 15 islets. In six of these experiments, intracellular recording from one cell showed that V_m and V_K always had the same periodicity. The mean value of the time difference between the commencement of the spike activity and the start of each oscillation in V_K was 1.6 ± 0.5 s for the experiment illustrated in Fig. 5. The mean amplitude of V_K for the experiments illustrated in this paper was 4.7 ± 1.3 mV. This signal represents an increase in $[K^+]_I$ of 1.5 ± 0.9 mM. The oscillations were often observed at various depths within the same islet. As the $[K^+]$-sensitive electrode was introduced deeper into the islet, the oscillations tended to increase in amplitude but always showed the same frequency. The oscillations in V_K were seen only in the

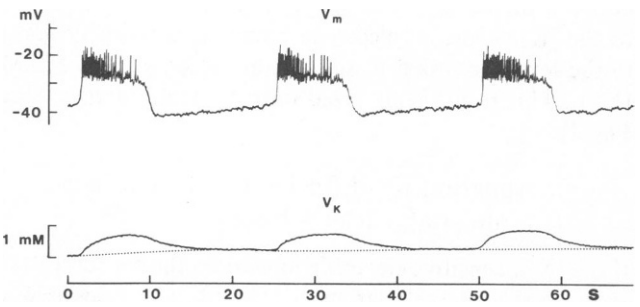

FIGURE 5 Simultaneous recordings in expanded time scale. V_m represents the membrane potential record from a cell 65 μm from the surface of the islet. V_K represents the $[K^+]$-sensitive microelectrode potential record made with the tip at a depth of 90 μm. Islet diameters were roughly 140, 250, and 300 μm. The concentration change was estimated as 0.8 mM ($[K^+]_o$ = 5 mM). Experiment in the presence of 11 mM glucose at 27°C.

presence of 11 and 16 mM glucose; these concentrations are known to induce bursts of electrical activity, at 27 or 37°C. The oscillations ceased when glucose was either removed from or augmented to 22 mM in the perifusion medium. Oscillations were never seen using nonselective microelectrodes placed in the islet interstitial space.

The time relationship between the simultaneously recorded membrane electrical activity and $[K^+]_I$ in the presence of 11 mM glucose at 27°C are compared in Fig. 5. It may be seen that the signal V_K (equivalent to a small concentration increase of ~0.6 mM) reached its maximum value at the end of the active phase of the burst. The return of V_K to the basal level was slower than the abrupt return of V_m to the membrane potential during the silent phase.

Effects of External Calcium on Glucose-induced Oscillatory Changes in $[K^+]_I$

The burst pattern of glucose-induced electrical activity is affected by $[Ca^{2+}]_o$. An increase of $[Ca^{2+}]_o$ increases the duration of the silent phase, decreases the active phase and the size of the membrane potential change in the transition from silent to active phase is also augmented (Atwater et al., 1980).

We have seen that in records of V_m (Fig. 4, upper trace) and V_K (Fig. 4, lower trace) made in the presence of 11 mM glucose Krebs solution with 2.5 mM Ca^{2+} at 37°C the oscillatory changes in V_K were in perfect phase with the bursts of electrical activity. Similar records were made in 7.5 mM $CaCl_2$ and they are shown in Fig. 6. The oscillatory changes in V_K are again in phase with the bursts of electrical activity. However, increasing Ca^{2+} caused an increase in the amplitude of V_K, from 3.7 ± 0.3 (n = 10 measurements in $[CaCl_2]_o$ = 2.5 mM) to 6.1 ± 1.3 mV (n = 7 measurements in $[CaCl_2]_o$ = 7.5 mM) as well as in the rate of rise of the signal, from 1.6 ± 0.1 to 2.6 ± 0.6 mV/s. The time course of the V_m and V_K oscillations shown in Fig. 6 *A*, although in phase, is fundamentally different. For example, the rising phase of V_K, which commences with the spike activity, reaches a peak value at the end of the active phase of the bursts and then it decays towards the base line. Also, while the return to the silent phase potential in the V_m record at 7.5 mM $CaCl_2$ takes less than 1 s, the average time for a 63% decrease in V_K towards the base line is 6 s.

The analysis of the time course of the $[K^+]$-sensitive microelectrode response for three bursts in Fig. 6 *A* (*a*, *b*, and *c*) is shown in part *B*. The continuous curves represent the tracing of the recorded V_K signal (taking the initial part of the corresponding burst as zero time). The points represent the best fit of a single exponential time course. The time for a 63% decrease in V_K (analysis of burst *a*) was 6.4 s. If one considers that the brief burst of spikes recorded in the presence of high Ca^{2+} (see Fig. 6 *B*) represents a sudden K^+ loading of the intercellular space, it is possible

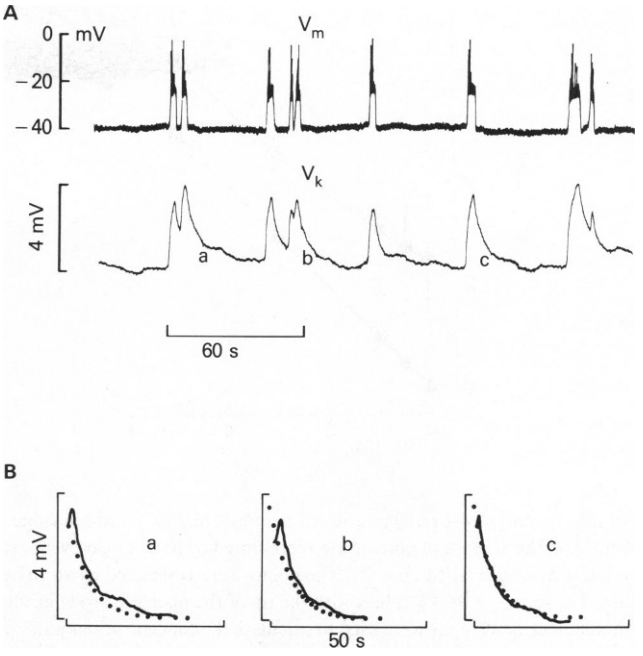

FIGURE 6 Simultaneous recordings of V_m and V_K in the presence of high Ca^{2+}. 2 min before the start of the record shown in part *A* external Ca^{2+} was increased from 2.56 to 7.5 mM. Mean V_K amplitude = 6.1 ± 1.3 mV representing a change in $[K^+]_I$ = 2.6 ± 0.6 mM; Mean dV_K/dt at the foot of the V_K oscillations = 2.6 ± 0.6 representing a change in $d[K^+]_I/dt$ = 0.9 $\mu M/cm^3 s$ (n = seven measurements). The analysis of the time course of V_K after bursts *a*, *b*, and *c* is shown in part *B*. For each graph: continuous lines represent a tracing of V_K taking the initial phase of each burst as time zero; points represent a single exponential decay calculated to fit the time course of the trace from burst *A*.

to estimate the apparent diffusion coefficient from the time course of the V_K signal (as illustrated in Fig. 6 *C*). Assuming that this time constant represents the time constant of K^+-unloading of the intercellular space then, using the time constant and the penetration depth from the experiment illustrated in Fig. 6 *B*, $D_{K,I}$ ($= \Delta r^2/\Delta T$) is calculated as 0.7×10^{-5} cm^2/s, about half that of $D_{K,o}$.

Intercellular Potassium Concentration in the Islet in the Absence of Glucose

The V_K records shown in Fig. 2, which were made in absence of glucose, indicate that the steady-state values of $[K^+]_I$ are larger than $[K^+]_o$. To determine the relationship between $[K^+]_I$ and $[K^+]_o$, six experiments were performed in which $[K^+]_o$ was varied between 0.1 and 5 mM in the absence of glucose. In Fig. 7, steady-state $[K^+]_I$ values calculated from steady-state V_K values recorded with the tip of the $[K^+]$-sensitive microelectrode at a depth of 84 μm inside the islet were compared with V_K values recorded with the tip of the electrode at a depth of 100 μm inside a block of 4% agar in place of the islet. It may be seen that the $[K^+]$ calculated from V_K reached the same steady-state value whether the tip was inside or outside the agar block (straight line) indicating that, under steady-state conditions, $[K^+]agar = [K^+]_o$. This result suggests that the

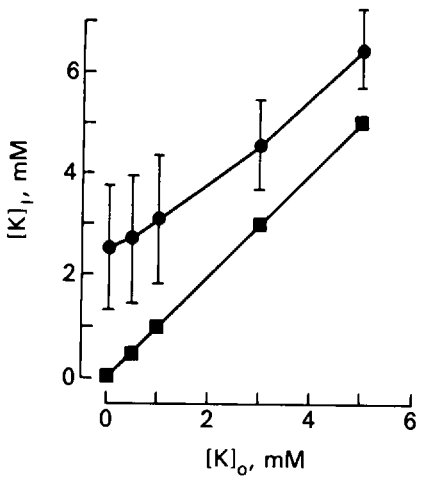

FIGURE 7 Intra-islet $[K^+]$ as a function of external $[K^+]$. Mean values of $[K^+]_I$ in the absence of glucose are represented by filled circles; vertical lines represent one SEM ($n = 7$). The points were connected by straight lines. The steady-state V_K values with the tip of the microelectrode inside a small block of 4% agar were used to calculate the concentrations plotted as filled squares. The straight line was drawn with a slope of one. Temperature 27°C.

properties of the $[K^+]$-sensitive electrode are not affected by introducing the tip 100 μm into the agar block. It is likely, therefore, that the difference in steady-state V_K values (records with the tip in the islet and outside the islet) shown in Fig. 2, is probably not caused by changes in the $[K^+]$-sensitive electrode properties during introduction into the islet tissue. The difference could represent a genuine K^+ concentration difference between a compartment inside the islet and the external solution.

Although for each islet tested the $[K^+]_I$ value obtained was greater than $[K^+]_o$, the size of the concentration difference, $[K^+]_I - [K^+]_o$, changed considerably from islet to islet and, for this reason the standard deviation associated with each value in Fig. 7 is large. The K^+ concentration difference was usually larger in the larger islets, even though the depth of penetration was 84 μm for all the islets used. It may be seen that the mean value of $[K^+]_I$ is always greater than $[K^+]_o$, the difference being statistically significant at $[K^+]_o$ below 2 mM.

DISCUSSION

This work reports the first use of $[K^+]$-sensitive microelectrodes in islets of Langerhans. The main experimental finding is that, both in absence or presence of glucose, the K^+-exchange between the intercellular space in the islet and the external medium is diffusion limited.

In the presence of 11 mM glucose the burst pattern is synchronous among most cells within an islet (Meda et al., 1984). Because of the restricted diffusion, the extra K^+-efflux during the repolarizing phase of the action potential, will induce a transient accumulation of K^+ in the intercellular space. Indeed, with the K^+sensitive microelectrodes within the islet tissue the amplitude of the oscillations in V_K was 4.7 ± 1.3 mV ($n = 24$ determinations in four different islets). These oscillations in V_K represent an oscillatory change in $[K^+]_I$ of 1.5 ± 0.9 mM. Simultaneous recording of V_K and V_m revealed that the changes in intercellular K^+ oscillate in phase with the bursts of electrical activity and at the same frequency.

Simultaneous measurements of insulin release from a single islet and electrical activity from a B-cell in that islet suggest that release of the hormone is also oscillatory and occurs during the active phase of the bursts (Atwater et al., 1979; Scott, Atwater, and Rojas, 1981). It is possible that the cations H^+, Ca^{2+}, and Zn^{2+}, which are released together with insulin (Howell and Tyhurst, 1982; Pace and Tarvin, 1983; Hutton, 1982; Hutton and Peshavaria, 1982), may cause oscillations in the potential of the liquid membrane electrode. Since the oscillations in V_K persisted at 27°C, when the insulin secretion is blocked (Atwater et al., 1984), the oscillations seen (Figs. 5 and 6) cannot be due to accumulation of ions or other substances being secreted with insulin.

Although the V_K signal is a positive potential and cannot be attributed to extracellular recording of the spike activity, control experiments showed that the response of the $[K^+]$-sensitive electrodes to a rectangular voltage pulse applied to the Krebs solution in the chamber was completed in <0.2 s and, therefore, V_K is too slow to represent the extracellular recording of a burst that had been filtered by the low frequency response of the $[K^+]$-sensitive electrode. Thus, the oscillatory changes in V_K measured in this work reflect genuine changes in $[K^+]_I$.

Diffusion Model

Diffusion into and out of the islet probably takes place through the intercellular spaces, representing ~2% of the islet cell volume (excluding the microcapillaries; Dean, 1973). Because of the small cell-to-islet volume ratio ($\sim 10^{-4}$), it is possible to treat the diffusion process within the intercellular space of the islet tissue, as radial diffusion in a continuous spherical volume. The analysis of the time course of the $[K^+]$-sensitive electrode response was carried out using a model that considers K^+ diffusion into and out of a spherical islet surrounded by an unstirred layer. In the computations, the thickness of the unstirred layer was adjusted to fit the time course of V_K with the $[K^+]$-sensitive electrode at the surface of the islet. The diffusion coefficient in the unstirred layer was taken as that for free diffusion ($D_{K,o}$ in Results). Diffusion within the islet tissue, although probably taking place in the intercellular spaces, was treated as radial diffusion in a continuous spherical medium. The apparent diffusion coefficient in this path ($D_{K,I}$ in Results) was adjusted to fit the main time course of V_K.

The equation for radial diffusion (for constant diffusion coefficient D) is

$$dC/dt = D\{d^2C/dr^2 + 2/r\,dC/dr\}. \quad (3)$$

Eq. 3 has been resolved by Crank (1956) for two special cases relevant to the model, namely, for the case of radial free diffusion through the unstirred layer (constant concentration outside; Eq. 6.18 in Crank, 1956) and, for the case where the concentration at the surface of a sphere of finite radius r is changing (Eq. 6.23 in Crank, 1956).

In this work, however, numerical methods were used to integrate Eq. 3 and calculate the time course of V_K. First, the equation was resolved for the diffusion of K^+ in the unstirred layer around the islet. Each calculated value $[K^+]_o$ was used to start the integration of Eq. 3 for diffusion within the sphere. To fit the experimental points (as illustrated in Fig. 3) a computer program was used. The algorithm for the numerical solution of the diffusion equation (Taylor et al., 1980) was added to a least-squares–fitting program as a subroutine. V_K was calculated with the Goldman-Hodgkin-Katz equation (see Methods) using the $[K^+]$-sensitive electrode parameters (V_o and SC) for the experiment and the computed concentration $[K^+]_I$ at a distance r from the surface of the islet. The model accurately reproduced the $[K^+]$-sensitive electrode responses recorded either with the tip outside or inside the islet tissue.

The main conclusion to be drawn from this analysis is that the apparent K^+-diffusion coefficient in the islet tissue is about half of that in free solution.

Intercellular K^+ Concentration in the Islet Tissue

It is generally agreed that in the absence of glucose the B-cell membrane potential is controlled by the total K^+-permeability of the membrane. Therefore $[K^+]_I$ must be determined by the relative size of four K^+ fluxes in and out of the intercellular space v (per unit area): (*a*) ${}_KJ_{c,v}$ from the cells to v; (*b*) ${}_KJ_{v,c}$ from v back into the cells; (*c*) ${}_KJ_{v,o}$ from v to the external medium and, (*d*) ${}_KJ_{o,v}$ from the external medium back into v.

For the rate of change of $[K^+]_I$ we can write

$$V_v/A_v\,(\mathrm{d}[K^+]_{I,t}/\mathrm{d}t) = ({}_KJ_{c,v} + {}_KJ_{o,v}) - ({}_KJ_{v,c} + {}_KJ_{v,o}), \quad (4)$$

where V_v/A_v represents the volume to surface ratio of the accumulation space (or the effective thickness of the space).

Addition of 22 mM glucose inhibits the overall K^+ permeability and depolarizes the B-cell membrane leading to continuous electrical activity. As the repolarization of the action potential is essentially due to a transient activation of voltage-gated K^+ channels, there is an extra K^+ efflux, ${}^*_KJ_{c,v}$, from the B-cells. Adding this term to Eq. 4 we get

$$V_v/A_v\,(\mathrm{d}[K^+]_{I,t}/\mathrm{d}t) = ({}_KJ_{c,v} + {}_KJ_{o,v} + {}^*_KJ_{c,v}) - ({}_KJ_{v,c} + {}_KJ_{v,o}). \quad (5)$$

Under steady-state conditions (continuous spike activity or no electrical activity)

$$\mathrm{d}[K^+]_{I,t}/\mathrm{d}t = 0.$$

Therefore,

$$\{{}_KJ_{c,v} + {}_KJ_{o,v} + {}^*_KJ_{c,v}\} - \{{}_KJ_{v,c} + {}_KJ_{v,o}\} = 0. \quad (6)$$

The tracer efflux data gives the total efflux, i.e. in Eq. 4 ${}_KJ_{c,v}$(absence of glucose) or in Eq. 5 ${}_KJ_{c,v} + {}^*_KJ_{c,v}$(presence of 22 mM glucose). In the absence of glucose the rate of ${}^{86}Rb^+$-outflow ($\sim 4 \times 10^{-4}$ s^{-1}) in both mouse (Dawson et al., 1983) and rat (Henquin, 1978) islets can be used to estimate ${}_KJ_{c,v}$. Taking the intracellular potassium concentration as 10^{-4} mol/cm^3 (Atwater et al., 1978), and the average cell radius as 6 μm, ${}_KJ_{c,v}$ is calculated as 8.3 pmol/(cm^2 s) (= cell volume/cell surface ratio × potassium concentration in the cells × rate of tracer K^+-outflow). This value is similar to the passive K^+-efflux measured in the squid giant axon (Hodgkin and Keynes, 1955).

Oscillatory Changes in $[K^+]$ Within the Islet Tissue

Atwater et al. proposed that in presence of glucose (in the range from 11 to 16 mM) the burst pattern of electrical activity in B-cells is controlled by the $[Ca^{2+}]_i$-activated K^+-permeability, which undergoes cyclic changes (Atwater et al., 1979*a*; Atwater, 1980; Atwater et al., 1983; Atwater et al., 1984). The spike activity during each active phase is mainly due to the activation of two voltage-gated channels, namely, the early Ca^{2+} channels and the delayed K^+ channels (Matthews and Sakamoto, 1975; Atwater et al., 1978; Ribalet and Beigelman, 1980). The high frequency of action potentials at the start of the plateau phase of the bursts is likely to induce a transient net efflux of K^+. Since diffusion in and out of the intercellular spaces in the islet tissue is restricted, the extra K^+-efflux associated with the electrical activity, is likely to increase $[K^+]_I$ (Frankenhaeuser and Hodgkin, 1956). The increased amplitude in $[K^+]_I$ and the increased rate of K^+-accumulation observed when Ca^{2+} was increased from 2.5 to 7.5 mM supports this notion, since increasing Ca^{2+} increases the frequency of the action potentials during the active phase of the burst (Atwater et al., 1980).

Assuming that the sum of the fluxes, ${}_KJ_{c,v}$, ${}_KJ_{v,c}$, ${}_KJ_{v,o}$, and ${}_KJ_{o,v}$ remains constant during glucose stimulation, and assuming that the recorded changes in V_K are due to ${}^*_KJ_{c,v}$, then the initial rate of change of $[K^+]_I$ is

$$V_v/A_v\,\{\mathrm{d}[K^+]_{I,t}/\mathrm{d}t\} = {}^*_KJ_{c,v} \quad (7)$$

In the presence of 11 mM glucose, ${}^*_KJ_{c,v}$ can be assumed equal to the average K^+ efflux of 5 pmol/cm^{2}s, or ~60% of the K^+ efflux measured in the absence of glucose (Henquin, 1978; Dawson et al., 1983). From time records of V_K

it is possible to estimate the extra K^+-efflux due to electrical activity. The mean value for the initial $d[K^+]_{I,t}/dt$ is $(0.8 \pm 0.1) \times 10^{-6}$ mol/cm^{3}s (24 measurements from four different islets). Eq. 7 can be used to calculate an effective thickness for the accumulation space, V_v/A_v, of 5×10^{-6} cm (or 50 nm).

As the average spike frequency during the active phase of each burst ranges between three and five spikes per second (Atwater and Beigelman, 1976; Meissner and Atwater, 1976), the extra K^+-efflux is calculated as 1 to 1.6 pmol/cm^2 per spike. This value falls in the range of the K^+-efflux per impulse measured in giant nerve fibers (Hodgkin, 1957).

The increased $[K^+]_I$ may increase the excitability of the central B-cells, similarly to the action of accumulated extracellular K^+ in other systems (Connors and Ransom, 1984), and this may in turn lower the threshold for glucose-stimulated electrical activity. Indeed, the centrally located B-cells have been observed to be more active in isolated islets (Kolod and Meda, 1981; Meda et al., 1984). In perifused islets, the majority of B-cells show a synchronous burst pattern of electrical activity in the presence of 11 mM glucose (Meda et al., 1984), while dye injection experiments indicate that the coupled B-cells are restricted to rather small domains (Michaels and Sheridan, 1981). The oscillations in $[K^+]_I$ may help to synchronize the bursting electrical activity among neighboring cell domains within the islet.

In summary, this study indicates that there is a significant accumulation of K^+ in the extracellular space of the islet. The diffusion of K^+ between this space and the perifusion medium is restricted, with a diffusion coefficient about half of that of K^+ in the external medium.

The authors are pleased to thank Dr. C. Edwards for reading and correcting the original manuscript. Thanks are also given to Dr. P. C. Croghan for many valuable discussions and suggestions. E. Perez-Armendariz was supported by Centro de Investigaciones y de Estudios Avanzados del Instituto Politecnico Nacional de Mexico.

The research was supported by the Medical Research Council, The British Diabetic Association, and the Science Research Council.

Received for publication 16 November 1984 and in final form 31 May 1985.

REFERENCES

Atwater, I. 1980. Control mechanisms for glucose induced changes in the membrane potential of mouse pancreatic B-cell. *Cienc. Biol. (Portugal).* 5:299–314.

Atwater, I., and P. M. Beigelman. 1976. Dynamic characteristics of electrical activity in pancreatic B-cells. Effects of calcium and magnesium removal. *J. Physiol. (Paris).* 72:769–786.

Atwater, I., C. M. Dawson, B. Ribalet, and E. Rojas. 1979*a*. Potassium permeability activated by intracellular calcium ion concentration in the pancreatic B-cell. *J. Physiol. (Lond.).* 288:575–588.

Atwater, I., C. M. Dawson, A. Scott, G. Eddlestone, and E. Rojas. 1980. The nature of the oscillatory behaviour in electrical activity from pancreatic B-cell. *Horm. Metab. Res.* (Suppl) 10:100–107.

Atwater, I., A. Goncalves, A. Herchuelz, P. Lebrun, W. J. Malaisse, E. Rojas, and A. Scott. 1984*a*. Cooling dissociates glucose-induced insulin release from electrical activity and cationic fluxes in pancreatic islets. *J. Physiol. (Lond.).* 348:615–627.

Atwater, I., B. Ribalet, and E. Rojas. 1978. Cyclic changes in potential and resistance of the B-cell membrane induced by glucose in islets of Langerhans from mouse. *J. Physiol. (Lond.).* 278:117–139.

Atwater, I., B. Ribalet, and E. Rojas. 1979*b*. Mouse pancreatic B-cells: tetraethylammonium blockage of the potassium permeability increase induced by depolarization. *J. Physiol. (Lond.).* 288:561–574.

Atwater, I., E. Rojas, and A. Scott. 1979*c*. Simultaneous measurements of insulin release and electrical activity from single micro-dissected mouse islets of Langerhans. *J. Physiol. (Lond.).* 291:57P.

Atwater, I., L. Rosario, and E. Rojas. 1983. Properties of the Ca-activated K-channel in pancreatic B-cells. *Cell Calcium.* 4:451–461.

Commission on analytical nomenclature. 1976. Recommendations for nomenclature of ion-selective electrodes. *Pure Appl. Chem.* 48:127–132.

Connors, B. W., and B. R. Ransom. 1984. Chloride conductance and extracellular potassium concentration interact to modify the excitability of rat optic nerve fibres. *J. Physiol. (Lond.).* 355:619–633.

Crank, J. 1956. The mathematics of diffusion. Clarendon Press, Oxford.

Dawson, C. M., P. C. Croghan, I. Atwater, and E. Rojas. 1983. Estimation of potassium permeability in mouse islets of Langerhans. *Biomed. Res.* 4:389–392.

Dean, P. M. 1973. Ultrastructural morphometry of the pancreatic B-cell. *Diabetologia.* 9:115–119.

Eddlestone, G. T., A. Goncalves, J. A. Bangham, and E. Rojas. 1984. Electrical coupling between B-cells in islets of Langerhans from mouse. *J. Membr. Biol.* 77:1–14.

Ferrer, R., B. Soria, C. M. Dawson, I. Atwater, and E. Rojas. 1984. Effects of Zn^{2+} on glucose-induced electrical activity and insulin release from mouse pancreatic islets. *Am. J. Physiol.* 246:C520–C527.

Frankenhaeuser, B., and A. L. Hodgkin. 1956. The after-effects of impulses in the giant nerve fibres of *Loligo*. *J. Physiol. (Lond.).* 131:341–376.

Goldman, D. E. 1943. Potential, impedance and rectification in membranes. *J. Gen. Physiol.* 27:37–60.

Henquin, J. C. 1978. D-glucose inhibits potassium efflux from pancreatic islet cells. *Nature (Lond.).* 271:271–273.

Hodgkin, A. L. 1957. Ionic movements and electrical activity in giant nerve fibres. *Proc. R. Soc. Lond. B. Biol. Sci.* 148:1–37.

Hodgkin, A. L., and B. Katz. 1949. The effect of sodium ions on the electrical activity of the giant axon of the squid. *J. Physiol. (Lond.).* 108:37–77.

Hodgkin, A. L., and R. D. Keynes. 1955. Active transport of cations in giant axons from *Sepia* and *Loligo*. *J. Physiol. (Lond.).* 128:28–60.

Howell, S. L. and M. Tyhurst. 1982. The insulin storage granule. *In* The Secretory Granule. Poisner and Trifaro, editors. Elsevier/North Holland Biomedical Press. Chapter 4. 155–172.

Hutton, J. C. 1982. The internal pH and membrane potential of the insulin secretory granule. *Biochem. J.* 204:171–178.

Hutton, J. C., and M. Dashavaria, M. 1942. Proton-translocating Mg^{2+}-dependent ATPase activity in insulin-secretory granules. *Biochem. J.* 204:161–170.

Kilb, K. H., and R. Stämpfli. 1974. A new stopcock for pharmacological purposes. *Naunyn-Schmiedebergs Arch. Pharmakol.* 285:293–295.

Kolod, E., and P. Meda. 1981. Influence of intra-islet environment on B-cell function. *Experiencia.* 37:650.

Matthews, E. K. and Y. Sakamoto. 1975. Electrical characteristics of pancreatic islet cells. *J. Physiol. (Lond.).* 246:421–437.

Meissner, H. P., and I. Atwater. 1976. The kinetics of electrical activity of B-cells in response to 'square wave' stimulation with glucose or glibenclamide. *Horm. Metab. Res.* 8:11–15.

Meda, P., I. Atwater, A. Goncalves, A. Bangham, L. Orci, and E. Rojas. 1984. The topography of electrical synchrony among B-cells in the mouse islet of Langerhans. *Quart. J. Exp. Physiol.* 69:719–735.

Michaels, R. L., and J. D. Sheridan. 1981. Islet of Langerhans: dye coupling among immunocytochemically distinct cell types. *Science (Wash. DC).* 214:801–803.

Pace, C. S., and J. T. Tarvin. 1983. pH modulation of glucose-induced electrical activity in B-cells: involvement of Na/H and HCO3/Cl antiportera. *J. Membr. Biol.* 73:39–49.

Ribalet, B., P. M. Beigelman. 1980. Calcium action potentials and potassium permeability activation in pancreatic B-cells. *Am. J. Physiol.* 239:C124–133.

Robinson, R. A., and R. H. Stokes. 1959. Electrolyte solutions. Butterworths, London.

Scott, A. M., I. Atwater, and E. Rojas. 1981. A method for the simultaneous measurement of insulin release and B-cell membrane potential in single mouse islets of Langerhans. *Diabetologia.* 21:470–475.

Taylor, R. E., F. Bezanilla, and E. Rojas. 1980. Diffusion models for the squid axon Schwann cell layer. *Biophys. J.* 29:95–118.

Thomas, R. C. 1978. Ion-sensitive intracellular microelectrodes. Academic Press, Inc., London.

Tsien, R. Y., and T. J. Rink. 1980. Neutral carrier ion selective microelectrodes for measurement of intracellular free-calcium. *Biochim. Biophys. Acta.* 599:623–638.